Yoon-Kyoung Cho<sup>1</sup> Suhyeon Kim<sup>2</sup> Kyusang Lee<sup>2</sup> Chinsung Park<sup>2</sup> Jeong-Gun Lee<sup>2</sup> Christopher Ko<sup>2</sup>

<sup>1</sup>School of Nano-Biotechnology and Chemical Engineering, UNIST, Ulsan, Republic of Korea <sup>2</sup>Bio & Health Group, Samsung Advanced Institute of Technology, Suwon, Republic of Korea

Received March 16, 2009 Revised June 26, 2009 Accepted June 30, 2009

# Research Article

# Bacteria concentration using a membrane type insulator-based dielectrophoresis in a plastic chip

We report an insulator-based (or, electrodeless) dielectrophoresis utilizing microfabricated plastic membranes. The membranes with honeycomb-type pores have been fabricated by patterning the SU-8 layer on a substrate which was pretreated with self-assembled monolayer of octadecyltrichlorosilane for the easy release. The fabricated membrane was positioned between two electrodes and alternating current field was applied for the particle trap experiments. The particle could be trapped due to the dielectrophoresis force generated by the non-uniformities of the electric fields applied through the membranes with pores. Simulations using CFD-ACE+(CFD Research, Huntsville, Alabama) suggested that the dielectrophoresis force is stronger in the edge of the pores where the field gradient is highest. The bacteria could be captured on the near edge of the pores when the electric field was turned on and the trapped bacteria could be released when the field was turned off with the release efficiency of more than  $93\pm7\%$ . The maximal trapping efficiency of  $66\pm7\%$  was obtained under the electric fields  $(E=128\,\mathrm{V/mm})$  and  $f=300\,\mathrm{kHz}$ ) when the dilute bacteria solution (Escherichia coli:  $9.3\times10^3\,\mathrm{cell/mL}$ ,  $0.5\,\mathrm{mS/m}$ ) flowed with a flow rate of  $100\,\mathrm{\mu L/min}$ .

# Keywords:

Bacteria concentration / Dielectrophoresis / Insulator-based dielectrophoresis / Microfabrication DOI 10.1002/elps.200900179



### 1 Introduction

Dielectrophoresis (DEP) has been employed to sort, manipulate, and concentrate a wide range of particle types including mammalian cells [1–5], bacteria [6–12], viruses [13–15], and DNA [16–18]. The majority of DEP studies reported in the literature employ micro-fabricated metallic electrodes. The DEP force was significantly enhanced in the microelectrode array-based system, thanks to the advancement of the micro fabrication technology.

Recently, alternative ways to construct DEP traps, namely insulator-based (or electrodeless) DEP, (iDEP) have been reported [6, 7, 12, 13, 18–23]. In iDEP chips, the DEP

Correspondence: Professor Yoon-Kyoung Cho, School of Nano-Biotechnology and Chemical Engineering, UNIST, Ulsan, 689-805, Republic of Korea

**E-mail:** ykcho@unist.ac.kr **Fax:** +82-52-217-2509

Abbreviations: AC, alternating current; DEP, dielectrophoresis; iDEP, insulator-based dielectrophoresis; ITO, indium tin oxide; ODC, octadecyltrichlorosilane; PC, polycarbonate; SAM, self-assembled monolayer

trap is formed by geometrical constrictions in insulating substrates (e.g. quartz [6, 7, 12, 13, 18], glass beads[20, 24], cyclo-olefin polymer [22], PMMA [21], and polycarbonate (PC)[23]) instead of metallic microelectrodes. A Non-uniform electric field is generated near the non-uniform structures made of insulating materials when an electric field is applied to remotely located electrodes. The DEP trap has been formed by using either packing materials [20, 24], single notch [6, 18], insulating post arrays [7, 12, 13], or membrane [23].

Chou et al., demonstrated concentration of Escherichia coli by iDEP chips made of PDMS by soft lithography techniques [6, 18]. The iDEP trap has a 4  $\mu$ m opening and 10  $\mu$ m depth and applies an alternating current (AC) electric field. Separation of *E. coli* from blood cells, electo-lysing of blood cells, and pre-concentration of DNA have been demonstrated using either PDMS or quartz-based iDEP chips even at high-salt buffer conditions (e.g.  $1 \times PCR$  buffer).

Cummings and co-workers developed iDEP chips, which have arrays of insulating posts inside microchannels [7, 12, 13, 19]. The iDEP chip has been employed to selectively trap and concentrate both live and dead *E. coli* and separate different species of live bacterial cells from water



using a direct current electric field [7, 12, 13, 19]. Mela *et al.*, reported reduced trapping voltage thresholds for the iDEP chips fabricated with cyclo-olefin polymer as compared with the previously reported glass-based iDEP chips [22].

Suehiro *et al.* [24] and Iliescu *et al.* [20] used a filter type device filled with glass beads for the trapping of yeast cells (*Saccharomyces cerevisae*). The glass beads packed between two electrodes induced non-uniformity of the electric fields and therefore the DEP force was stronger than the drag force exerted by the liquid flow, which could trap particles. In both reports, the flow rate was relatively higher compared with the experiments performed with 2-D DEP chips[1–5].

Lee *et al.* [23] showed that nanoparticles array could be formed on PC membrane by positive DEP. Nanoparticles could be trapped near the pores with 100, 200, or 400 nm diameter on the PC membrane whose backside has indium tin oxide (ITO) electrodes. The positive DEP on nanoporous membranes was demonstrated at no flow condition and the bacteria-trapping experiments were not tried.

We report an alternative pore-type iDEP technique utilizing microfabricated plastic membranes with specific pore geometry. The bacteria could be captured on the near edge of the pores when the AC field was turned on by positive DEP. The positive DEP phenomena were observed between 10 kHz and 1 MHz and the maximum trapping efficiency was obtained at 300 kHz when the frequency of the electric field was varied from 10 kHz to 10 MHz. The trapping efficiency of  $66\pm7\%$  was obtained under the electric fields ( $E=128\,\mathrm{V/mm}$ ,  $f=300\,\mathrm{kHz}$ ) when the dilute bacteria solution ( $E.~coli:~9.3\times10^3\,\mathrm{cell/mL},~0.5\,\mathrm{mS/m}$ ) flowed with a flow rate of  $100\,\mu\mathrm{L/min}$ . When the AC field

was turned off, the trapped bacteria could be released with the release efficiency of more than  $93 \pm 7\%$ .

### 1.1 Principles of iDEP

Dielectrophoretic force arise when a polarizable object is subjected to a non-uniform electric field and can be written to a first approximation as [6]

$$F_{\text{DEP}} = \alpha(\omega)E\nabla E \tag{1}$$

Where  $\alpha(\omega)$  is the polarizability of the object at the angular frequency,  $\omega$ , and E is the applied external electric field. For a spherical object of radius a, the DEP force may be solved analytically in a form:

$$F_{\rm DEP} = 2\pi a^3 \varepsilon_m \text{Re} \left( \frac{\varepsilon_p^* - \varepsilon_m^*}{\varepsilon_p^* - 2\varepsilon_m^*} \right) \nabla E^2$$
 (2)

Where  $\varepsilon_{\rm P}^*$  and  $\varepsilon_{\rm m}^*$  are the complex permittivity of the dielectric particle and the medium, respectively. Depending on the differences in the complex permittivity of particle and the medium, the object may be either trapped to (positive DEP,  ${\rm Re}(\varepsilon_{\scriptscriptstyle p}^*-\varepsilon_{\scriptscriptstyle m}^*)>0)$  or repelled from (negative DEP,  ${\rm Re}(\varepsilon_{\scriptscriptstyle p}^*-\varepsilon_{\scriptscriptstyle m}^*)<0)$  the high-field gradient region.

As there is geometric constriction in the *z*-direction as shown in Fig. 1A, the DEP forces can be written as

$$F_{DEP} = \alpha(\omega) E \frac{\partial E}{\partial z} \tag{3}$$

where z is the direction of the applied external electric field E. In the previously reported post-type DEP traps, there is only 1-D geometric constriction in the x-direction as shown in

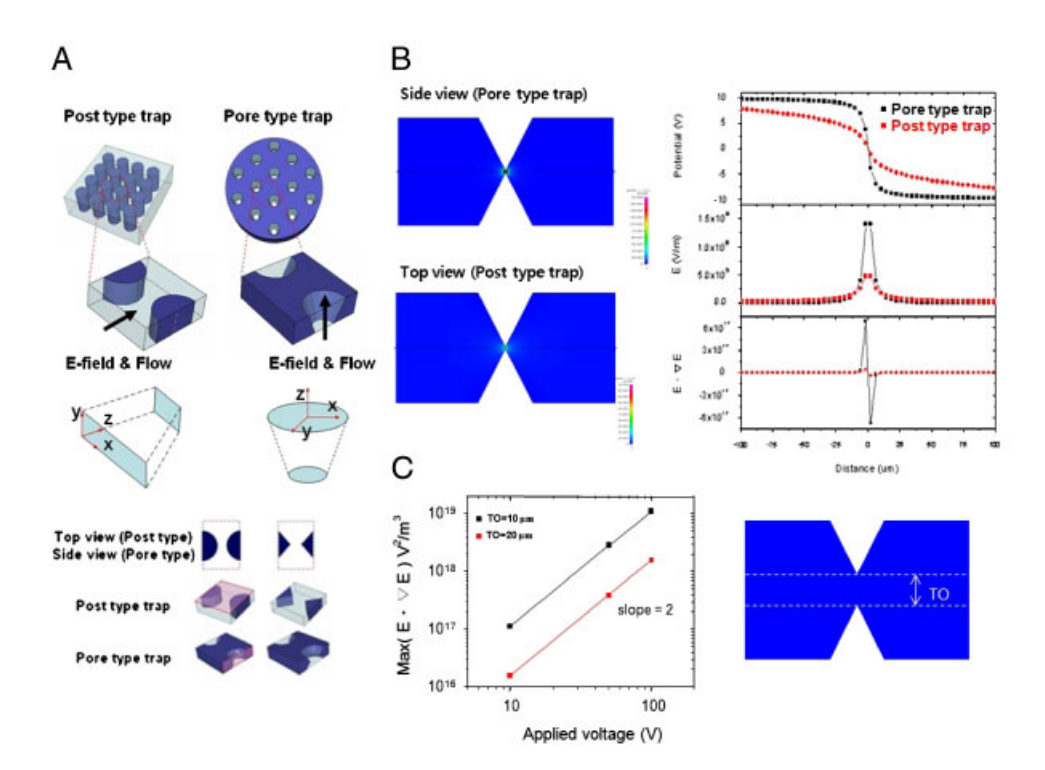


Figure 1. (A) Schematic diagram showing concept of post-type versus pore-type iDEP trap. (B) The simulation shows that the maximum dielectric force normalized to the polarizability, Max  $(E \bullet \nabla E)$ . is significantly enhanced for pore-type iDEP compared with the conventional post-type iDEP. (C) The smaller trap opening, the higher DEP force. The DEP force is proportional to the applied voltage with the slope of 2 in the log-log plot of Max  $(E \bullet \nabla E)$  versus applied voltage as expected.

Fig. 1A. However, there are 2-D geometric constrictions both in x- and y-direction in the proposed pore-type DEP traps. The simulations using CFD-ACE<sup>+</sup> (CFD Research, Huntsville, Alabama) suggested that the DEP forces in pore-type traps were significantly higher than the post-type traps as shown in Fig. 1B. The trap opening is defined as the smallest distance between post and the smallest diameter of the pore for the post- and the pore-type trap, respectively. In both cases, the maximum field density was at the tips of the constrictions.

As one can expect, the DEP force was significantly enhanced at smaller trap openings as shown in Fig. 1C. For example, the maximum DEP force for the pores with 10 and  $20\,\mu m$  of pore opening was 139 and 18 times stronger than the pore with  $50\,\mu m$  of trap opening, respectively. However, the pressure drop could also be significant to adversely affect the liquid flow or even to break the membranes as the trap opening becomes smaller. The robustness of the membrane also depends on the opening factors as well as the pore dimension [25].

# 2 Materials and methods

### 2.1 Fabrication of pore-type iDEP chip

Figure 2A shows the schematic illustration of the fabrication process of pore-type iDEP chips. The SU-8 (Microchem®,

SU-8 2100,  $\epsilon'=4.1, \epsilon''=0.015$ ) layer patterned on a substrate was easily released by the use of an intermediate layer of self-assembled monolayer (SAM) of octadecyltrichlorosilane (ODC). The SAM of ODC was prepared by immersing a clean silicon substrate in a 100 mM ethanol solution of ODC for 60 min. The substrate was cleaned with ethanol for 10 min and followed by baking in an oven at 110°C for 45 min. Before exposure to the ODC solution, the surface was cleaned with piranha solution,  $H_2SO_4$ : $H_2O_2$  in 3:1 volume ratio, and thoroughly washed using deionized water. The contact angle after the surface modification was  $112\pm2^\circ$ .

Next, SU-8 2100 photoresist was spin coated at 1400 rpm to prepare the microstructures with a height of 200 µm. Soft baking was carried out at 65°C for 5 min, followed by slow heating from 65 to 95°C with a heating speed of 2°C/min, and held at 95°C for 20 min before it cooled down to 65°C with a cooling rate of 1°C/min. UV exposure dose was 390 mJ/cm<sup>2</sup>. Post-exposure baking was carried out at 75°C and heating time was 15 min.

After the patterning of the SU-8 layer, the substrate was rinsed with isopropyl alcohol and buffered oxide etchant for 1 min each to release the SU-8 membranes. The contact angle of the SU-8 membrane was 72–92°. The hydrophobic nature of the membrane surface adversely affects the liquid flow through the holes in the membranes [26]. After the plasma treatment (PDC-002, Harrick Plasma, direct current 29.6 W) for 30 s, the membrane became hydrophilic (the

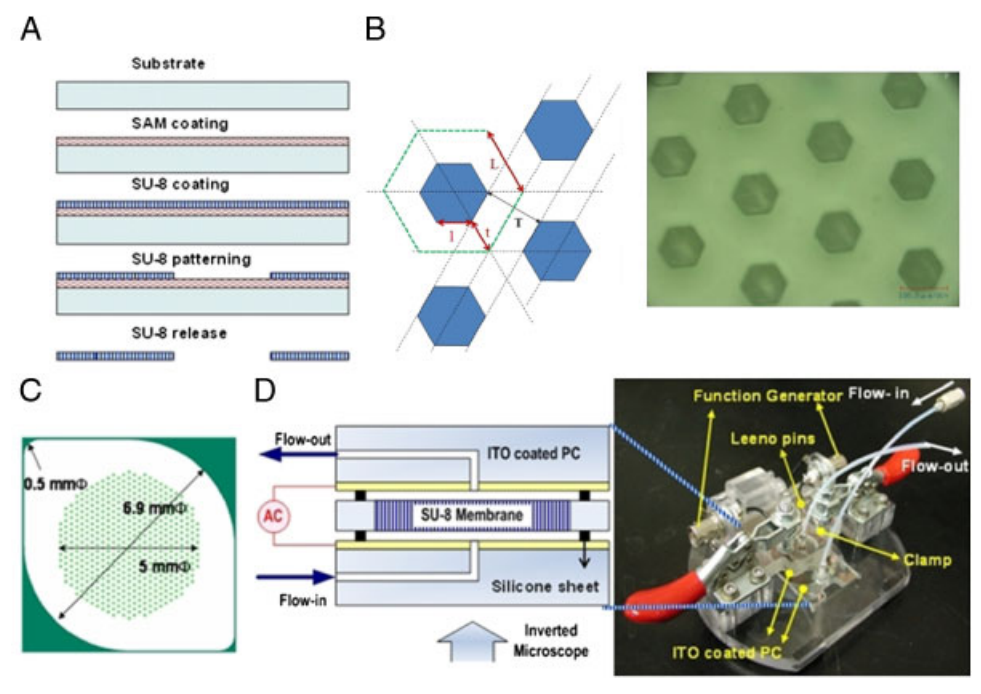


Figure 2. (A) Schematic diagram of the fabrication process of SU-8 membrane chips. (B) Optical micrograph showing the top view of the chip with honeycomb-type pores. The side length of the hexagon shape pore (I) is 50  $\mu$ m. The side length of the unit cell (L) is t+1, 115  $\mu$ m, and the thickness of the wall between pores (T) is  $2t \times \cos(30^\circ)$ , 112.6  $\mu$ m, when t is 65  $\mu$ m. (C) Mask layout of a pore-type iDEP chip. The chip has circular (diameter = 5 mm) region with 517 pores. (D) Experimental setup for the visualization of bacteria trapping by pore-type iDEP. The microfluidic channels are machined on PC parts. The top and bottom surfaces in parallel with SU-8 membranes are coated with ITO to be used as electrodes. Leeno pins are used to make good contacts between Bayonet Neill–Concelman connectors and ITO-coated surfaces.

contact angle was  $18\pm2^{\circ}$ ) and kept in deionized water for the following experiments.

Figure 2B shows the top view of the chip with honeycomb-type pores. The side length of the hexagonal pore was  $50\,\mu m$  and the thickness of the wall between pores was  $112.6\,\mu m$ . Figure 2C shows an example of a mask layout of pore-type iDEP chip. The diameter of the membrane area was  $5\,m m$  and 517 pores were located with a honeycomb pattern. The void fraction in the membrane was 18.7%.

# 2.2 Microfluidic and electric interface jig for poretype iDEP operation

A custom-built microfluidic and electric interface jig as shown in Fig. 2D was used to introduce cell solution to the chip, apply an electric field, and visualize the bacteria trapping. The pore-type iDEP chip made of SU-8 membrane is located between silicone sheets machined to fit into the jig. The fluidic channels are machined in PC parts and the top and bottom surfaces in parallel with SU-8 membranes that are coated with ITO to be used as electrodes.

The interface jig was designed to be compatible with an inverted microscope (Eclipse TE300, Nikon) equipped with a cooled CCD camera (Photometrics Quantix 57) for visualization. The Leeno pins are used to make good contacts between Bayonet Neill–Concelman connectors and ITO-coated surfaces when the interface jig is clamped tightly. Sinusoidal waveforms up to 160 V at various frequencies raging from 100 Hz to 10 MHz were applied using a function generator (Agilent, 33120A) and linear voltage amplifier (FLC electronics AB, F1020). After the assembly, the distance between the electrodes was 1.25 mm.

Fluids were introduced into the chip from 1 mL syringes using a syringe pump (Cavro XP 3000, Tecan) and the flow process was digitally controlled using a custom-designed LabVIEW program. Before the bacteria solution was introduced to the chip, the system was flushed and primed with 1–3 mL of media with the same conductivity as the bacteria solution. The bacteria solution was introduced to the chip at various flow rates ranging from 50 to 500  $\mu L/min$  and monitored by microscope. The concentration of each aliquot of bacteria sample was taken from the outlet tubing before the electric field was applied, while the electric fields were on, and after the electric field was removed and measured to calculate the capture efficiency.

### 2.3 Bacteria preparation

E. coli (ATCC# 11775) was grown in brain-heart infusion broth (Becton Dickinson Co.) at 37°C and the cells were harvested after 18 h and washed three times with washing buffer. The concentration was adjusted to an OD of 1.0 at 600 nm. The washing buffer was diluted PBS buffer with

the conductivity adjusted to a desired value (e.g. 0.5 mS/m) using a conductivity meter (Horiba, D-54).

For the visualization of the cells under fluorescence microscope, bacteria were stained using the live/dead BacLight Bacterial viability kit (Molecular probes, USA) according to the manufacturer's instruction. SYTO 9 penetrates the bacteria membranes and stains the cells green, whereas propidium iodide only penetrates the cells with damaged membranes, and the combination of the two dyes makes the bacteria red.

For the quantification of the bacteria concentration, non-labeled bacteria were used and the concentration was measured by colony-counting method using 3 M Petrifilm.

# 3 Results and discussion

Bacteria-trapping experiments using the proposed pore-type iDEP phenomena were carried out with the SU-8 membranes with honeycomb-type pores as shown in Fig. 2B. The pore-type iDEP chip was assembled in the microfluidic and electric interface jig shown in Fig. 2D and an AC electric field (128 V/mm, 300 kHz) was applied between the ITO electrodes for the bacteria-trapping experiments.

Figure 3 shows the SEM images of the cross-sectional view of the fabricated pores. The measured height of the pore was 160  $\mu m$  and the distance between pores was 118  $\mu m$ . The trap openings for the top and bottom were approximately 75 and 50  $\mu m$ , respectively. Before the poretype iDEP trap by flowing the bacteria solution (*E. coli*:  $1\times 10^7$  cell/mL, 0.5 mS/m) with a flow rate of 100  $\mu L/min$ , the membrane surface was clean without particles as shown in Figs. 3A and B.

After 1 min of bacteria trapping, the SEM images of the SU-8 membranes show many bacteria on the surfaces of pores and membrane surfaces as shown in Figs. 3C and D. The SEM image was taken with the dried membrane after the AC field was turned off. The cross-sectional view of the pore of the pore-type iDEP chip used in the experiments was similar to the rectangular shape except that the pores in the surface originally faced the silicon substrate and released by rinsing with ethanol have relatively sharp and narrowed rims as shown in Fig. 3A. The SEM image shows that the trap opening of this side is 50 µm compared with 75 µm in the surface-facing air during the fabrication process.

One of the difficulties to prepare SU-8 membranes comes from the fact that the cross-linked SU-8 binds well to Si. It is not possible to mechanically release the SU-8 structures without damaging, unless a release layer is used. Previous studies have shown that the SU-8 layer could be released by using a Cr-Au-Cr sacrificial layer. The sacrificial layer could be removed by wet etching but it is time consuming [27]. In this study, we have used a hydrophobic SAM of ODC as an intermediate layer for easy release of the SU-8 membrane.

Figure 4 shows the fluorescence microscope images taken when the bacteria solution (*E. coli*:  $1 \times 10^7$  cell/mL,

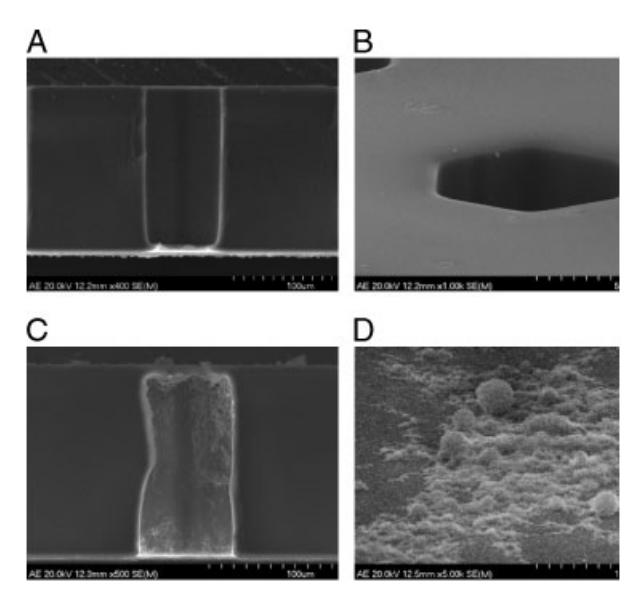


Figure 3. (A) SEM image of the cross-sectional view of the SU-8 membrane before the DEP experiments. (B) The top view of the membrane showing the hexagonal shape of the pore before the DEP experiments. (C) SEM image of the cross-sectional view of the SU-8 membrane after the bacteria concentration by poretype iDEP. (D) The top view of the membrane showing many bacteria after the concentration by pore-type iDEP phenomena.

 $0.5\,\text{mS/m})$  flowed with a flow rate of  $100\,\mu\text{L/min}$ . Figure 4A is the image taken prior to the electric field being turned on. One minute after applying an alternating electric field (E = 128 V/mm and f = 300 kHz), the bacteria are trapped on the edge of the pores as shown in Fig. 4B. Figure 4C is an enlarged diagram to show the detailed view of the trapped bacteria near the entrance of the pore. When the electric field was turned off, the trapped bacteria were released as shown in Fig. 4D (see also the movie shown in the Supporting Information).

It is noteworthy that the trapping experiments could be conducted at a relatively high flow rate, \emph{e.g.} 100  $\mu L/min.$  In most of the experiments performed with the 2-D DEP chips, the flow velocity was less than 1 mm/s. The membrane-type DEP device can be advantageous because the flow rate could be higher even if the flow velocity is the same.

Figure 5A shows the frequency response of the *E. coli* solution under the AC field applied to the conventional microfabricated metal electrode array-based DEP chips. The positive DEP was observed between 10 kHz and 1 MHz and the capture efficiency was the maximum at about 1 MHz when the conductivity of the media was  $0.2 \, \text{mS/m}$ .

Figure 5B shows fluorescence intensity increase due to the capture of the bacteria on the proposed membrane-type DEP device as a function of the applied frequency. The positive DEP phenomena were observed between 10 kHz and 1 MHz. The maximum trapping efficiency was obtained at 300 kHz. This is the similar frequency response that could be obtained with conventional metal electrode array-based DEP chips as shown in Fig. 5A.

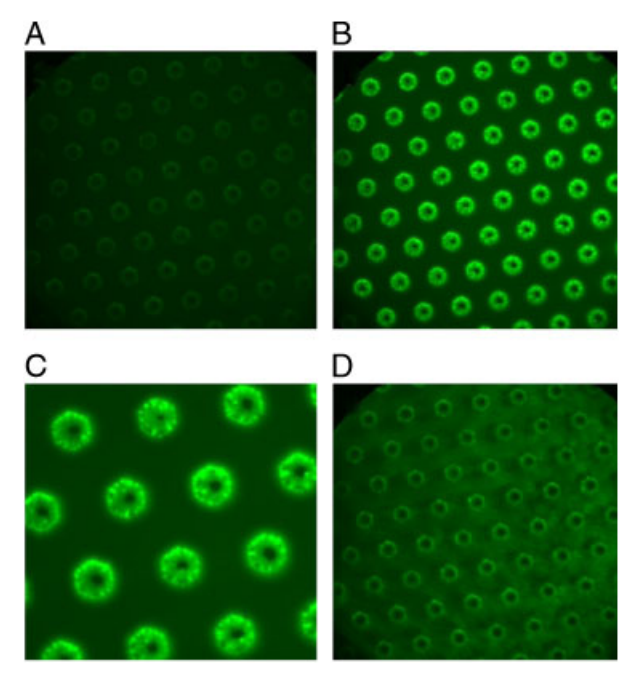


**Figure 4.** Microscope images taken during the trapping and release of *E. coli* by pore-type iDEP. *E. coli* is labeled with live/dead BacLight Bacterial viability kit (Molecular probes). (A) Before the electric field is turned on. (B) One minute after applying an alternating electric field ( $E=128\,\text{V/mm}$  and  $f=300\,\text{kHz}$ ). (C) Enlarged picture of the image shown in Fig. 4B showing each bacterium trapped on the edge of the pores. (D) *E*-field is turned off and bacteria are released.

The joule heating could be an important issue for the biological applications. In the current experimental condition, the Joule heating was not observed. The reason could be the following. The *E*-field that we apply (128 V/mm) was much smaller than the *E*-field applied to typical metal electrode-based DEP chips where typically 15 V was applied between electrodes separated by 15  $\mu$ m (1000 V/mm). Furthermore, we have used the AC field with frequency 300 kHz and the medium has relatively small conductivity (0.5 mS/m).

Figure 5C shows the concentration of each aliquot of 50 μL sample during the DEP experiments using the membrane-type DEP device. A dilute bacteria solution (E. coli:  $9.3 \pm 0.3 \times 10^3$  cell/mL, 0.5 mS/m) was injected with a flow rate of 100 µL/min. For the quantification of the bacteria concentration, non-labeled bacteria were used and the concentration of each aliquot of 50 µL sample was measured by colony counting using 3 M Petrifilm. The average concentration measured from three replicates of serially diluted samples was used for the analysis and the CV% was less than 7%. As soon as the electric field (E = 128 V/mm and  $f = 300 \,\mathrm{kHz}$ ) was turned on at 2 min, the bacteria are captured on the edge of the pores as shown in Fig. 3C and the concentration of the aliquot dropped dramatically. When the electric field is turned off at 5 min, the captured E. coli is released and the concentration of the aliquot increased a lot. An alternating electric field was applied from 2 to 5 min. The

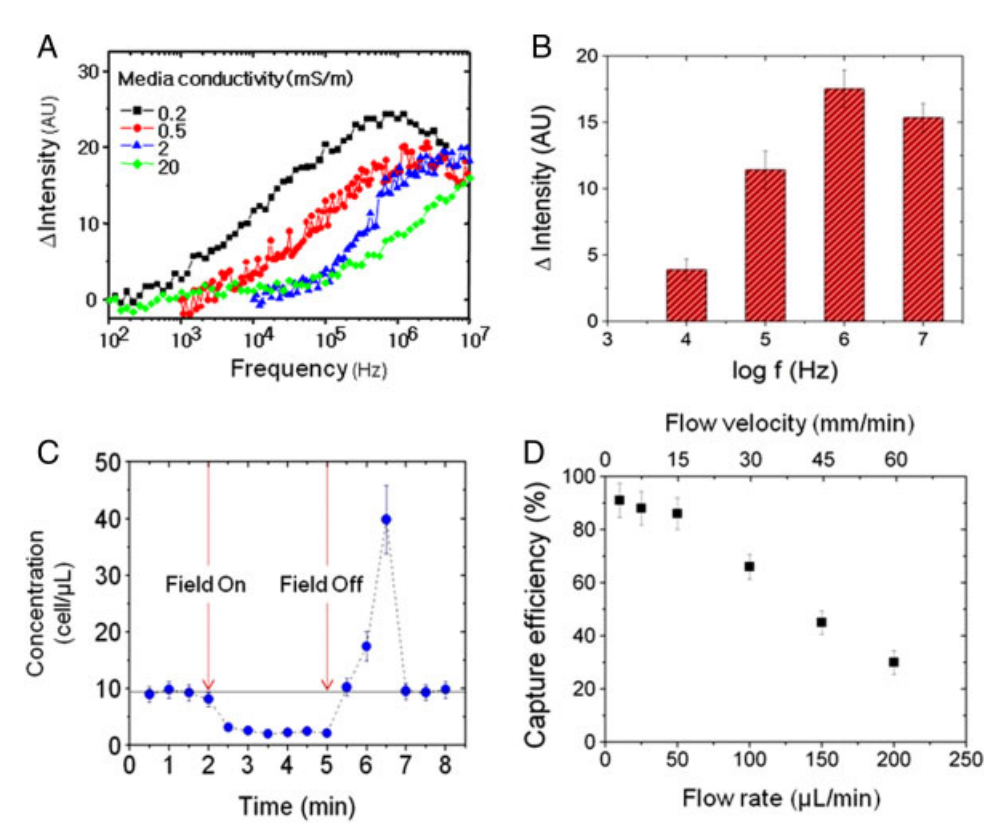


Figure 5. (A) The effect of the frequency, 10 kHz–10 MHz, on the capture efficiency of *E. coli* as a function of the media conductivity. The positive DEP was observed when the alternate electric field (20 V) was applied between electrodes separated by 15 μm. (B) The effects of the frequency on the capture efficiency of *E. coli* solution  $(1.0 \times 10^7 \text{ cell/mL}, 0.5 \text{ mS/m})$  on the proposed membrane-type DEP device. The maximum trapping efficiency was obtained at 300 kHz. Alternate electric field (128 V/mm) was applied for 60 s and the increase of the fluorescence intensity was measured. (C) The bacteria concentration of each 50 μL from the outlet was measured by using colony-counting method. The electric field (128 V/mm, 300 kHz) was applied for 3 min. The captured bacteria were released as soon as the electric field was turned off. (D) The bacteria-capture efficiency was obtained as a function of the flow rates from 10 to 250 μL/min.

number of captured bacteria was about  $4.3\pm0.3\times10^4$  and the released bacteria were about  $4.0\pm0.3\times10^4$ . The maximal trapping efficiency of  $66\pm7\%$  was obtained under the electric fields ( $E=128\,V/mm$  and  $f=300\,kHz$ ) when the dilute bacteria solution ( $E.\,coli:~9.3\times10^3\,cell/mL,~0.5\,mS/m$ ) flowed with a flow rate of  $100\,\mu L/min$ . The release efficiency was more than  $93\pm7\%$ .

In the proposed membrane-type DEP device, the flow rate is highest at the center of the pores where the DEP force is weak. However, the bacteria could be trapped at smaller flow rates where the DEP force is higher than the hydrodynamic force. Figure 5D shows the capture efficiency as a function of the flow rate. The capture efficiency higher than 80% was obtained at the average flow velocity less than 10 mm/s. However, the capture efficiency dropped to 30% when the flow velocity is higher than 50 mm/s.

# 4 Concluding remarks

An iDEP chip utilizing microfabricated plastic membranes has been designed and evaluated for the bacteria capture. The simulation suggests that the DEP forces of the poretype traps are larger than the post-type traps. The cross-sectional area is larger than the post-type traps and therefore dielectrophoretic trapping of the bacteria could be demonstrated at a relatively high flow rate (e.g.  $100\,\mu\text{L/min}$ ). The positive DEP was observed between  $10\,\text{kHz}$  and  $1\,\text{MHz}$  when E. coli solution in the media with the conductivity of  $0.5\,\text{mS/m}$  was used. This is similar condition that can be achieved with the conventional electrode-based DEP chips. When compared with the size-based separation using conventional filters, a small pore size is not necessary and thus issues such as clogging or fracture due to pressure drop could be less problematic.

The authors have declared no conflict of interest.

# 5 References

- [1] Holmes, D., Green, N. G., Morgan, H., IEEE Eng. Med. Biol. Mag. 2003, 22, 85-90.
- [2] Gray, D. S., Tan, J. L., Voldman, J., Chen, C. S., Biosens. Bioelectron. 2004, 19, 771–780.

- [3] Gascoyne, P., Mahidol, C., Ruchirawat, M., Satayavivad, J., Watcharasi, P., Becker, F. F., Lab Chip 2002, 2, 70–75.
- [4] Becker, F., Wang, X., Huang, Y., Pethig, R., Vykoukal, J., Gascoyne, P., Proc. Natl. Acad. Sci. USA 1995, 92, 860–864.
- [5] Xu, C., Wang, Y., Cao, M., Lu, Z., Electrophoresis 1999, 20, 1829–1831.
- [6] Chou, C.-F., Zenhausern, F., IEEE Eng. Med. Biol. Mag. 2003, 22, 62–67.
- [7] Lapizco-Encinas, B. H., Simmons, B. A., Cummings,
  E. B., Fintschenko, Y., Anal. Chem. 2004, 76, 1571–1579.
- [8] Li, H., Bashir, R., Sensor. Actuat. B 2002, 86, 215-221.
- [9] Prinz, C., Tegenfeldt, J. O., Austin, R. H., Cox, E. C., Sturm, J. C., Lab Chip 2002, 2, 207–212.
- [10] Huang, Y., Ewalt, K. L., Tirado, M., Haigis, R., Forster, A., Ackley, D., Heller, M. J. et al., Anal. Chem. 2001, 73, 1549–1559.
- [11] Yang, J. M., Bell, J., Huang, Y., Tirado, M., Thomas, D., Forster, A. H., Haigis, R. W. et al., Biosens. Bioelectron. 2002, 17, 605–618.
- [12] Lapizco-Encinas, B., Simmons, B., Cummings, E., Fint-schenko, Y., *Electrophoresis* 2004, *25*, 1695–1704.
- [13] Lapizco-Encinas, B. H., Davalos, R. V., Simmons, B. A., Cummings, E. B., Fintschenko, Y., J. Microbiol. Methods 2005, 62, 317–326.
- [14] Morgan, H., Hughes, M. P., Green, N. G., Biophys. J. 1999, 77, 516–525.
- [15] Hughes, M., Morgan, H., Rixon, F., *Biochim. Biophys. Acta* 2002, *1571*, 1–8.

- [16] Asbury, C. L., Diercks, A. H., Engh, G. v. d., Electrophoresis 2002, 23, 2658–2666.
- [17] Ying, L., White, S. S., Bruckbauer, A., Meadows, L., Korchev, Y. E., Klenerman, D., Biophys. J. 2004, 86, 1018–1027.
- [18] Chou, C.-F., Tegenfeldt, J. O., Bakajin, O., Chan, S. S., Cox, E. C., Darnton, N., Duke, T. et al., Biophys. J. 2002, 83, 2170–2179.
- [19] Cummings, E. B., Singh, A. K., Anal. Chem. 2003, 75, 4724–4731.
- [20] Iliescu, C., Xu, G. L., Loe, F. C., Ong, P. L., Tay, F. E. H., Electrophoresis 2007, 28, 1107–1114.
- [21] Chuang, K.-C., Chu, L.-Y., Jiang, M.-S., Chuang, T.-H., Fu, C.-C., Fan, S.-K., MicroTAS, Tokyo, Japan 2006, pp. 398–400.
- [22] Mela, P., Berg, A. v. d., Fintschenko, Y., Cummings, E. B., Simmons, B. A., Kirby, B. J., *Electrophoresis* 2005, 26, 1792–1799.
- [23] Lee, H. J., Yasukawa, T., Suzuki, M., Taki, Y., Tanaka, A., Kameyama, M., Shiku, H. et al., Sensor. Actuat. B Chem. 2008, 131, 424–431.
- [24] Suehiro, J., Zhou, G., Imamura, M., Hara, M., IEEE Trans. Ind. Appl. 2003, 39, 1514–1521.
- [25] Yang, X., Yang, J. M., Tai, Y.-C., Ho, C.-M., Sensor. Actuat. 1999, 73, 184–191.
- [26] Hsiai, T. K., Cho, S. K., Yang, J. M., Yang, X., Tai, Y.-C., Ho, C.-M., J. Fluid Eng. 2002, 124, 1053–1055.
- [27] Sidler, K., Mechanical Engineering, Technical University of Denmark (DTU) 2006, pp. 7–18.